JOURNAL
OF THE AMERICAN CHEMICAL SOCIETY

VOLUME 100, NUMBER 12 JUNE 7, 1978

Energy Transfer in Excited Ionic Species. Rates and Mechanism of Dimerization of Protonated Amines with Their Neutral Bases

Paul V. Neilson, Michael T. Bowers,* Marian Chau, William R. Davidson, and Donald H. Aue

Contribution from the Department of Chemistry, University of California, Santa Barbara, California 93106. *Received April 25, 1977*

Abstract: The dimerization reactions of the ammonium ions NH_4^+, $CH_3NH_3^+$, $(CH_3)_2NH_2^+$, and $(CH_3)_3NH^+$ with their neutral bases have been studied over the pressure range of 1×10^{-4} to 3×10^{-3} Torr and for temperatures of 200–400 K using ion cyclotron resonance spectroscopy. Preliminary data on larger amines at 300 K are also reported. The mechanism $AH^+ + A \rightarrow (A_2H^+)^*$ (k_f), followed by $(A_2H^+)^* \rightarrow AH^+ + A$ (k_b) or $(A_2H^+)^* + A \rightarrow A_2H^+ + A$ (k_s), has been confirmed for all systems. The rate of the overall phenomenological reaction $AH^+ + 2A \rightarrow A_2H^+ + A$ (k_2) exhibits a continuous transition from third-order to second-order kinetics over the entire pressure range. From plots of $1/k_2$ vs. $(A)^{-1}$ the rate constants k_f and $k_3 = k_f k_s/k_b$ are determined. The data are discussed both in terms of a dynamic model, in which energy is not randomized in the $(A_2H^+)^*$ complex, and in terms of a statistical model, in which it is assumed energy is randomized in the $(A_2H^+)^*$ complex. From these data alone it is not possible to tell which model is correct.

Introduction

The determination of the detailed mechanism of chemical reactions has long been one of the primary goals in chemistry. In neutral systems, the mechanism of energy disposal or energy transfer during a reaction has been widely studied. Perhaps the most successful technique has been to measure branching ratios (or stabilization/decomposition ratios) as a function of pressure and temperature.[1-3] These data have been understood in terms of the RRKM approach[4] to chemical reactions and present one of the great success stories in chemistry. In the past several years these "classic" approaches have been augmented by results from single collision molecular beam studies.[5] The single collision experiments allow the determination of microscopic mechanisms that are usually not averaged over angle and often are not averaged over thermal energy.

In ion chemistry, there has been very little experimental work published on the types of studies that have laid the mechanistic foundation of energy transfer in neutral gas-phase chemistry.[1-3] There has been one photoionization study of the reactions in ethylene by Gill et al.[6] and a number of papers on the mechanism of dimerization reactions by several laboratories.[7-9] Recently, an RRKM analysis of several of these dimerization reactions has been given by Olmstead et al.[10] In this paper, we present a very detailed investigation of the dimerization reactions of the ammonium ions, NH_4^+, $CH_3NH_3^+$, $(CH_3)_2NH_2^+$, and $(CH_3)_3NH^+$ with their neutral bases. These systems are particularly well suited for detailed study because there is only one reaction channel—formation of the proton bound dimer. The technique used is ion cyclotron resonance (ICR) spectroscopy. The reactions are studied over the pressure range of $1 \times 10^{-4} \leq P \leq 3 \times 10^{-3}$ Torr and at temperatures of $195 \leq T \leq 400$ K. A thorough discussion of the mechanistic implications of the results will be given and comparisons made with other work on these reactions.

Experimental Section

The experiments reported here were run on the UCSB drift cell ICR spectrometer which has been previously described.[11] Pressure was measured with an MKS Baratron 145 capacitance manometer. Thermal transpiration corrections were applied as previously discussed.[11b] Drift times were measured by trapping plate ejection.[12] Most experiments were run at electron beam energies near threshold (9–11 eV), although higher energies were used in several cases. Temperatures were measured with a copper-constantan thermocouple bolted to the resonance trapping plate and either a millivolt potentiometer or an internally compensated digital thermometer was used for readout. Details of the temperature dependent cell are given elsewhere.[11b,13] The amines used were either the highest purity commercially available or were obtained from recrystallization of the hydrochloride.

The reactions were all run at constant magnetic field with the sensitivity of the marginal oscillator calibrated using a Q-spoiler device.[14] This procedure greatly simplifies the analysis and eliminates potential problems of differential reactivity or ion loss.

The problem of ion loss to the drift electrodes at high pressures was considered. At all times, the pressures were maintained below those predicted for onset of this phenomenon, using the criteria of Ridge and Beauchamp.[15]

0002-7863/78/1500-3649$01.00/0

Kinetic Analysis

The phenomenological reactions occurring in the ICR cell are

$$A + e^- \rightarrow A^{+\cdot} + 2e^- \quad (1a)$$

$$A^{+\cdot} + A \rightarrow AH^+ + (A - H) \quad (1b)$$

$$AH^+ + 2A \rightarrow A_2H^+ + A \quad (1c)$$

$$A_2H^+ + 2A \rightarrow A_3H^+ + A \quad (1d)$$

where A = NH_3, CH_3NH_2, $(CH_3)_2NH$, and $(CH_3)_3N$. This paper will be primarily concerned with the pair of reactions (1b and 1c) and will focus attention on reaction 1c. The trimerization reaction (1d) is observed for A = CH_3NH_2 and $(CH_3)_2NH$ at low temperatures and high pressures. Results for A = $(CH_3)_2NH$ are reported here. Significant trimerization is not observed for A = NH_3 or $(CH_3)_3N$ under the conditions of the experiments described in this paper.

Reaction 1c can be written in terms of the detailed mechanism

$$AH^+ + A \xrightarrow{k_f} (A_2H^+)^* \quad (2a)$$

$$(A_2H^+)^* \xrightarrow{k_b} AH^+ + A \quad (2b)$$

$$(A_2H^+)^* + A \xrightarrow{k_s} A_2H^+ + A \quad (2c)$$

This energy-transfer mechanism was first suggested by Bohme et al.,[7] who studied dimerization reactions of small ions with the parent gases and has subsequently been applied by Anicich and Bowers[8] to dimerization reactions in benzene and 1,1-difluoroethylene, and by Meot-Ner and Field[9] to dimerization reactions of certain of the amines reported here. If the apparent second-order rate constant, k_2, for formation of A_2H^+ is defined in

$$d(A_2H^+)/dt = k_2(AH^+)(A) \quad (3)$$

then it follows from mechanism 2 that

$$k_2 = \frac{k_f k_s(A)}{k_b + k_s(A)} \quad (4)$$

if $(A_2H^+)^*$ is assumed to be in a steady state. If the third-order rate constant for formation of A_2H^+ is defined by

$$k_3 \equiv \frac{dk_2}{d(A)}\bigg|_{\lim(A)\rightarrow 0} = \frac{k_f k_s}{k_b} \quad (5)$$

then substitution into (4) and rearrangement yields

$$\frac{1}{k_2} = \frac{1}{k_3(A)} + \frac{1}{k_f} \quad (6)$$

Hence, a plot of $1/k_2$ vs. $1/(A)$ should yield a straight line of slope $1/k_3$ and intercept $1/k_f$ if the microscopic mechanism 2 is operative.

The unimolecular rate constant, k_b, can be determined from (5) using measured values of k_f and k_3 and a calculated value of k_s. In this work, it is assumed that k_s can be accounted for accurately by the ADO collision theory.[16] This assumption is reasonable because the excited ion $(A_2H^+)^*$ has only one dissociation channel, the thermoneutral path 2b, and a collision that removes even a small amount of energy from $(A_2H^+)^*$ will make this channel endothermic. The parent neutral polyatomic molecules should be very efficient stabilizers, and hence k_s should be near the collision limit.

In the drift cell ICR, integrated power absorption coefficients are measured rather than ion concentrations.[17] Thus, these quantities must be related to ion intensities if one is to use the kinetic analysis developed in the beginning of this section. What is needed are expressions that will allow determination of the apparent second-order rate constant, k_2, as a function of concentration, (A), using the measured integrated power absorption of ions AH^+ and A_2H^+, that is, expressions for the power absorption of a reactive secondary ion, AH^+, and a nonreactive tertiary ion, A_2H^+. (The slow trimerization of A_2H^+ in CH_3NH_2 and $(CH_3)_2NH$ is easily corrected for.) Since pressure is varied over a wide range, these power absorption expressions have to be general. Neither low pressure nor high pressure limits are suitable. Such expressions were first derived by Comisarow[18] and later rederived in a more convenient form by Kemper.[19] Kemper's expressions are given below:

Reactive secondary ion

$$A_s = \frac{KS^+_0 I}{m_s\xi_s(I-J)}\left\{\exp(-J\tau'_s)\left[\frac{1-\exp(-J\tau_s)}{J} - \frac{(1-\exp(-J-\xi_s)\tau_s)}{J+\xi_s}\right] + \frac{\xi_s\exp(-I\tau'_s)}{I-J-\xi_s}\left[\frac{1-\exp(-I\tau_s)}{I} - \frac{(1-\exp(-J-\xi_s)\tau_s)}{J+\xi_s}\right]\right\} \quad (7)$$

Nonreactive tertiary ion

$$A_t = \frac{KS^+_0 IJ}{m_t\xi_t(I-J)}\left\{\left[\tau_t - \frac{(1-\exp(-\xi_t\tau_t))}{\xi_t}\right]\left[\frac{I-J}{IJ}\right] - \frac{\exp(-I\tau'_t)}{I^2(I-\xi_t)}[\xi_t(1-\exp(-J\tau_t)) - I(1-\exp(-\xi_t\tau_t))] + \frac{\exp(-J\tau'_t)}{J^2(J-\xi_t)}[\xi_t(1-\exp(-J\tau_t)) - J(1-\exp(-\xi_t\tau_t))]\right\} \quad (8)$$

where A is the integrated power absorption coefficient, K is a constant related primarily to the amplitude of the observing field, S^+_0 is the initial secondary ion concentration, τ and τ' are the ion reaction times in the source-drift and resonance regions of the spectrometer, respectively, ξ is the collision frequency, I is the first-order rate constant for reaction 1b, and J is the first-order rate constant for reaction 1c. The subscripts s and t represent secondary (AH^+) and tertiary (A_2H^+) ions, respectively. The quantity of interest, $J = k_2(A)$, is to be determined from a measurement of A_s and A_t. By taking the ratio of A_s to A_t, the constants K and S^+_0 are eliminated. The rate constants I are taken from the literature values.[20] These rates are assumed to be independent of temperature. However, even if they change by a factor of 2 over the temperature range of interest, the values of k_f and k_3 would be essentially unchanged. The reaction times are measured. The collision frequencies, ξ, are measured from ICR line widths,[15,17] with an example given in Figure 1a. These quantities are shown to depend substantially on temperature; hence, they were remeasured each time the temperature was changed. An example is given in Figure 1b. The resulting equation for the ratio of A_s/A_t is complex and cannot be solved analytically for the rate constant J. An iterative method was used where J would be guessed, A_s/A_t calculated and compared with experiment, and then the guessed J modified, etc. This procedure quickly yielded values of k_2 vs. (A) for the experiment of interest.

The reaction 1d is a reactive tertiary ion to a quaternary ion process requiring further kinetic analysis to obtain absolutely accurate answers. Such expressions are available but cumbersome.[19] One can, however, obtain a very close estimate of the rate constant as a function of pressure using the secondary ion to tertiary ion analysis given above. All that is needed is to substitute the experimental value of the pressure dependent second-order dimerization rate constant for I, the appropriate

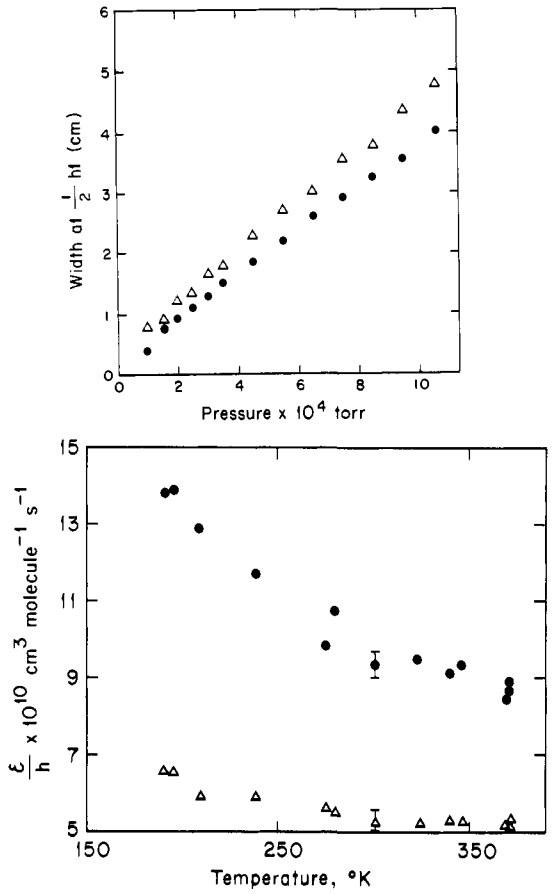

Figure 1. (a, top) Plot of the full resonance line width at half height vs. pressure for the $(CH_3)_3NH^+$ (●) and $[(CH_3)_3N]_2H^+$ (△) ions at 302 K in $(CH_3)_3N$. (b, bottom) Plot of the momentum transfer rate constant, ξ/n, vs. temperature for the $(CH_3)_3NH^+$ (●) and $[(CH_3)_3N]_2H^+$ (△) ions in $(CH_3)_3N$.

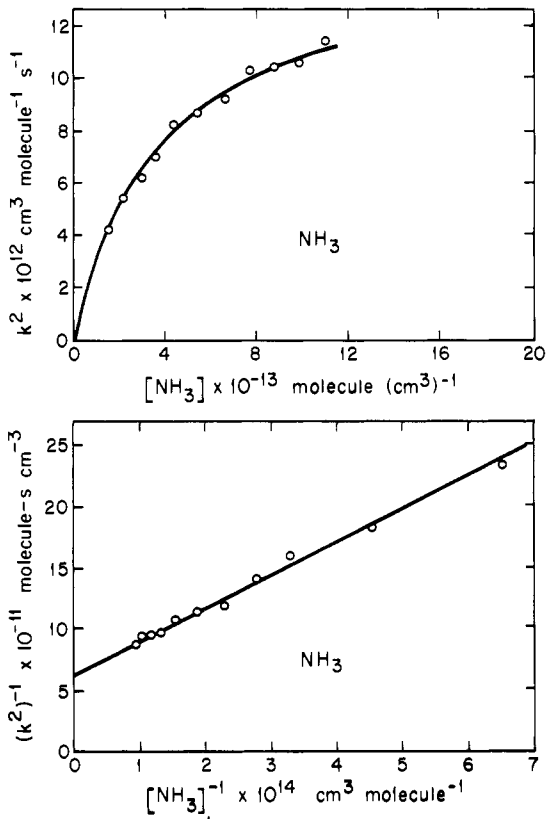

Figure 2. (a, top) Plot of the apparent second-order dimerization rate constant, k_2, vs. $[NH_3]$ at 213 K. (b, bottom) Plot of $1/k_2$ vs. $[NH_3]^{-1}$ at 213 K. The straight line in (b) is a least-squares fit of the data points. The values of k_f and k_3 determined from the intercept and slope of this line produce the solid curve in (a) when substituted in eq 4.

values of the ξ_s, and calculate J which would then correspond to the trimerization process 1d.

Results

A typical plot of line width vs. pressure for $(CH_3)_3N$ at 302 K is given in Figure 1a. From this data, it is straightforward to obtain the momentum transfer rate constant, ξ/n.[15,17] The values of ξ/n obtained at a series of temperatures are given in Figure 1b. Similar experiments were performed for all species. It is interesting to note that the values of ξ/n obtained are ~30% lower than predicted by ADO theory. The relative values of ξ for the monomer and dimer are accurately predicted by the Langevin theory, however.[21]

Figures 2–5 give experimental plots of k_2 vs. (A) and $1/k_2$ vs. $1/(A)$ for NH_3, CH_3NH_2, $(CH_3)_2NH$, and $(CH_3)_3N$. These are typical data taken at 302 K for the alkylamines and 213 K for NH_3. Clearly, all of the data fit the form expected from the energy-transfer mechanism suggested in the kinetic analysis section. Graphs such as these were used to obtain k_3 and k_f. By calculating k_s from ADO theory,[16] it is possible to obtain k_b. The values of k_3 and k_f obtained in this way are plotted as a function of temperature for the alkylamines in Figures 6–8. The ammonia data are summarized in Table I. The experiments on ammonia were very difficult because the intensity of the dimer ion never exceeded a few percent of the monomer intensity even at highest pressures and lowest temperatures. Hence, the data showed much more scatter than the alkylamine data.

The trimerization reaction 1d was studied in dimethylamine using the method described in the kinetic analysis section. Plots of k_2 vs. $((CH_3)_2NH)$ and $1/k_2$ vs. $((CH_3)_2NH)^{-1}$ are given in Figure 9. Clearly, the trimerization reaction qualitatively obeys the same mechanism as the dimerization reactions.

Table I. Experimental Rate Constants for the Dimerization Reaction of NH_4^+ in NH_3[a]

T, K	$k_f \times 10^{11}$,[b] cm^3 s^{-1}	$k_s \times 10^9$,[c] cm^3 s^{-1}	$k_3 \times 10^{25}$,[d] cm^6 s^{-1}
213	0.15	2.11	0.39
278	0.27	1.92	0.086
302	0.17	1.90	0.064

[a] The rate constants are defined in eq 2 and 5. [b] Determined from the intercept of plots similar to that in Figure 2b. Uncertainties in these data could be as large as a factor of 2 or 3. [c] Calculated from ADO theory.[16] [d] Determined from the slope of plots similar to that in Figure 2b. Uncertainties in these data could be as large as a factor of 2 or 3.

Preliminary data have been taken on a number of larger amines near room temperature. The values of k_3 and k_f for these systems are summarized in Table II. The data for NH_3 and the methylamines is included for comparison. All of the data for the larger amines fit the energy-transfer mechanism proposed for NH_3 and the methylamines, yielding plots qualitatively similar to those given in Figures 2–5. Rate constants for the trimerization reaction in $(CH_3)_2NH$ are collected in Table III at several temperatures.

One final point should be mentioned about the data before a discussion of them is begun. At the lowest pressures experimentally obtainable, with a measurable dimer peak, the observed value of k_2 appeared to be lower than expected from extrapolation of the higher pressure data. The effect was most apparent in the $1/k_2$ vs. $(A)^{-1}$ plots. When the AH^+ formation rate constant of reaction 1b was included in the kinetics, the deviation was substantially reduced. It is our opinion that the

Table II. Experimental Rate Constants for the Dimerization of Various Ammonium Ions in Their Parent Amines at 302 K (Rate Constants Defined in Eq 2 and 5)

Amine	$k_f \times 10^{11}$,[a] $cm^3\ s^{-1}$	k_f/k_{ADO}[b]	$k_s \times 10^9$,[c] $cm^3\ s^{-1}$	$k_3 \times 10^{25}$, $cm^6\ s^{-1}$	
				This work[d]	MF[e]
NH_3	0.17	8.0×10^{-4}	1.90	0.064	~0.03
CH_3NH_2	2.1	0.012	1.49	1.8	~0.2
$(CH_3)_2NH$	5.5	0.037	1.28	10.7	~0.3
$(CH_3)_3N$	3.3	0.026	1.10	12.4	
$C_2H_5NH_2$	9.5	0.067	1.35	17	
n-$C_3H_8NH_2$	17	0.140	1.19	75	
$(C_2H_5)_2NH$	10	0.083	1.10	28	
i-$C_4H_9NH_2$	16	0.13	0.95	198	

[a] Determined from the intercept of plots like those in Figures 2b-5b. These data are uncertain as much as ±40% except for NH_3 which may be in error by a factor of 2 or 3. [b] Approximately equal to the probability of forming a long-lived $(A_2H^+)^*$ complex per collision. [c] Calculated from ADO theory.[16] [d] Determined from the slope of plots like those in Figures 2b-5b. These data are uncertain by about ±20% except for NH_3, which may be in error by a factor of 2 or 3. [e] Meot-Ner and Field.[9]

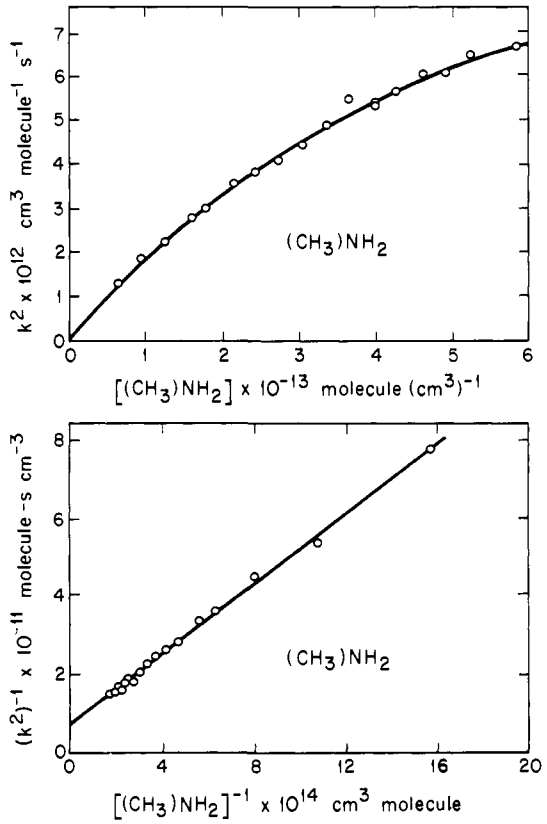

Figure 3. (a, top) Plot of the apparent second-order dimierization rate constant, k_2, vs. $[CH_3NH_2]$ at 302 K. (b, bottom) Plot of $1/k_2$ vs. $[CH_3NH_2]^{-1}$ at 302 K. The straight line in (b) is a least-squares fit of the data points. The values of k_f and k_3 determined from the intercept and slope of this line produce the solid curve in (a) when substituted in eq 4.

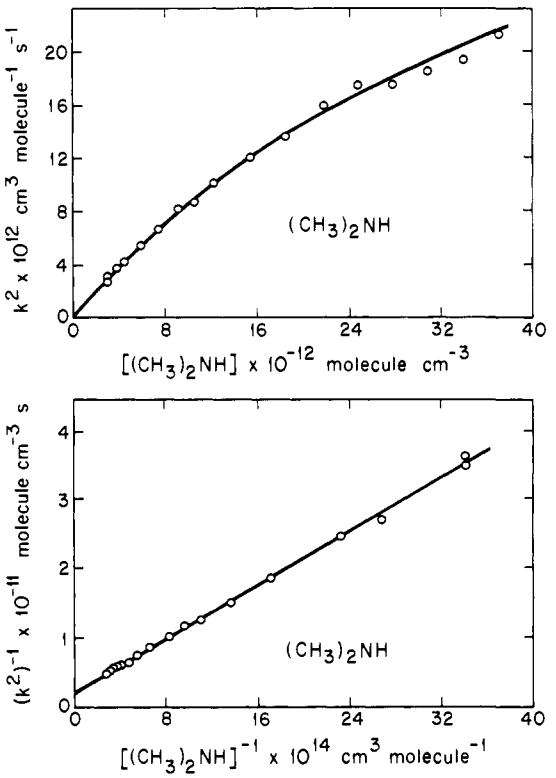

Figure 4. (a, top) Plot of the apparent second-order dimerization rate constant, k_2, vs. $[(CH_3)_2NH]$ at 302 K. (b, bottom) Plot of $1/k_2$ vs. $[(CH_3)_2NH]^{-1}$ at 302 K. The straight line in (b) is a least-squares fit of the data points. The values of k_1 and k_3 determined from the intercept and slope of this line produce the solid curve in (a) when substituted in eq 4.

remaining deviation at lowest pressures is due either to vibrational energy in the newly formed AH^+ ion or kinetic energy in this ion obtained from the observing field. Both of these effects should significantly reduce the observed value of k_2. When the pressure is increased to a point where the AH^+ ions have undergone several collisions, plots of $1/k_2$ vs. $(A)^{-1}$ are linear in all cases. We are convinced that this phenomenon in no way affects the results presented here or the discussion given in the following section.

Discussion

One of the most interesting results obtained in these studies is the apparent experimental value of k_f, the rate constant associated with the formation of a long-lived complex (see Table II), and the dependence of k_f on temperature. There are at least two ways to view the data. The first assumes the $1/k_2$ vs. $(A)^{-1}$ plots remain linear to $(A) = \infty$. This procedure yields the data for k_f summarized in Table II for T 302 K. This interpretation suggests that k_f bears little relationship to a collision rate constant and other factors must determine its magnitude and its dependence on temperature. The second interpretation assumes the $1/k_2$ vs. $(A)^{-1}$ plots are really not linear and they only appear linear over the limited pressure range studied. Hence, extrapolation to $(A) \rightarrow \infty$ gives misleading results concerning the true magnitude of k_f. Such an interpretation is implicit in a recent RRKM theory analysis of these reactions.[10] The gist of the RRKM argument is that k_b is pressure dependent and such a dependence produces curvature in the $1/k_2$ vs. $(A)^{-1}$ plots. Presumably some curvature should occur in these plots in the pressure range reported here, but it may be so slight as to be undetectable. The two interpretations will be handled sequentially.

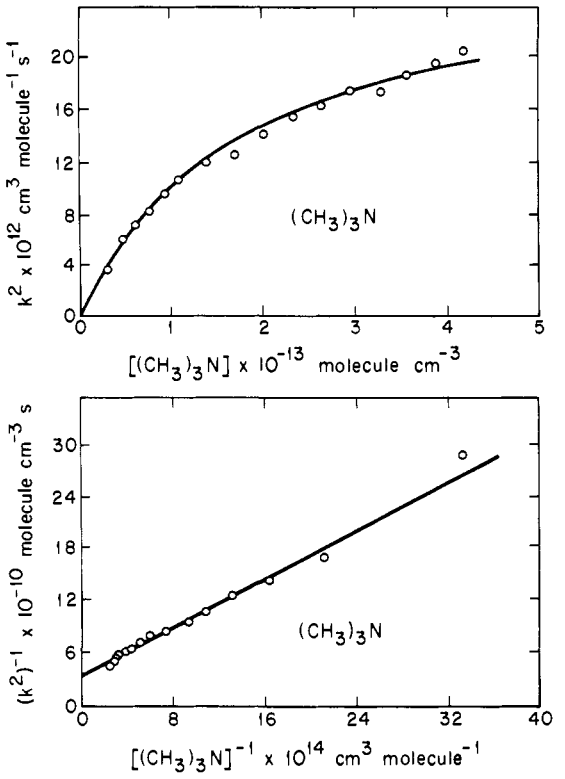

Figure 5. (a, top) Plot of the apparent second-order dimerization rate constant, k_2, vs. $[(CH_3)_3N]$ at 302 K. (b, bottom) Plot of $1/k_2$ vs. $[(CH_3)_3N]^{-1}$ at 302 K. The straight line in (b) is a least-squares fit of the data points. The values of k_f and k_3 determined from the intercept and slope of this line produce the solid curve in (a) when substituted in eq 4.

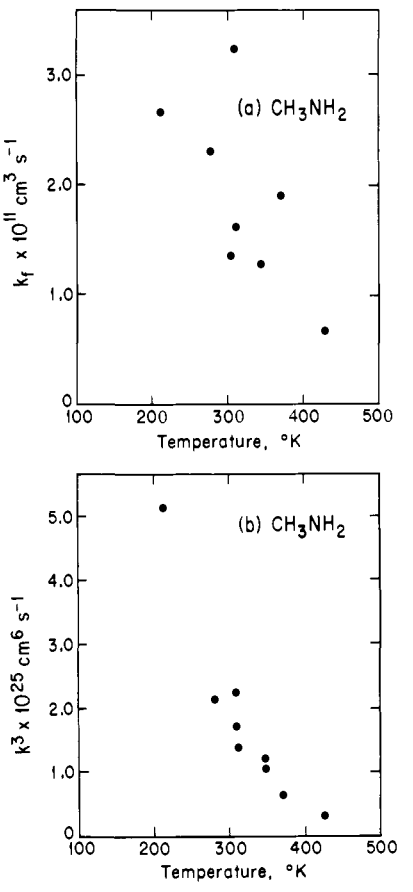

Figure 6. CH_3NH_2: (a, top) plot of k_f vs. T; (b, bottom) plot of k_3 vs. T.

Table III. Experimental Rate Constants for the Trimerization Reaction of $[(CH_3)_2NH]_2H^+$ in $(CH_3)_2NH$ (Rate Constants Defined in Eq 2 and 5)

T, K	$k_f \times 10^{11}$,[a] cm^3 s^{-1}	$k_s \times 10^9$,[b] cm^3 s^{-1}	$k_3 \times 10^{25}$,[c] cm^6 s^{-1}	$k_b \times 10^{-4}$,[d] s^{-1}
196	19	1.29	29	8.6
281	2.6	1.20	3.4	9.1
303	1.8	1.19	1.5	14

[a] Determined from the intercept of plots similar to that in Figure 9b. Uncertainties could be as large as ±50%. [b] Calculated from ADO theory.[16] [c] Determined from the slope of plots similar to that in Figure 9b. Uncertainties could be as large as ±30%. [d] Calculated from the relationship $k_b = k_f k_s / k_3$.

1. The Dynamical Model. First, it will be assumed that the extrapolation method yields reliable values of k_f. Consider the room temperature data of Table II. The values of k_f range from 1.7×10^{-12} cm^3/s for NH_3 to 1.7×10^{-10} cm^3/s for n-$C_3H_8NH_2$. The probability that a given collision will form a collision complex is given by the ratio k_f/k_{ADO}, where k_{ADO} is the collision rate constant.[16] The values of these probabilities range from 8.0×10^{-4} (NH_3) to 0.01–0.04 (methylamines) to 0.1–0.2 (larger amines). Hence, for NH_4^+/NH_3, only one collision in 1500 forms a long-lived complex capable of being stabilized in the ICR. As the amine increases in mass and molecular complexity, this probability increases but never exceeds ~1 in 5. Said in other words, there are at least two kinds of collisions between the ammonium ions and the neutral amines: in one set (the majority) the collision complex is very short lived while in a second set (the minority) a long-lived complex is formed capable of being stabilized in the ICR. Collision complexes of the "short-lived" variety would never be stabilized in the ICR while the complexes of the "longer-

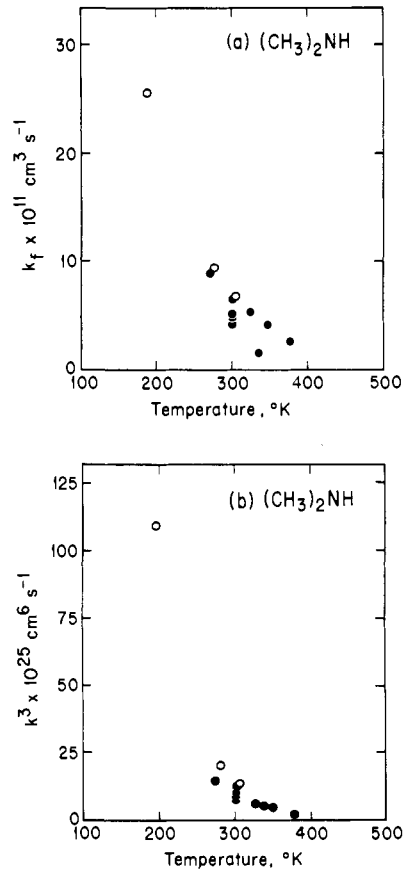

Figure 7. $(CH_3)_2NH$: (a) plot of k_f vs. T; (b) plot of k_3 vs. T. The open circles represent data corrected for the trimerization reaction.

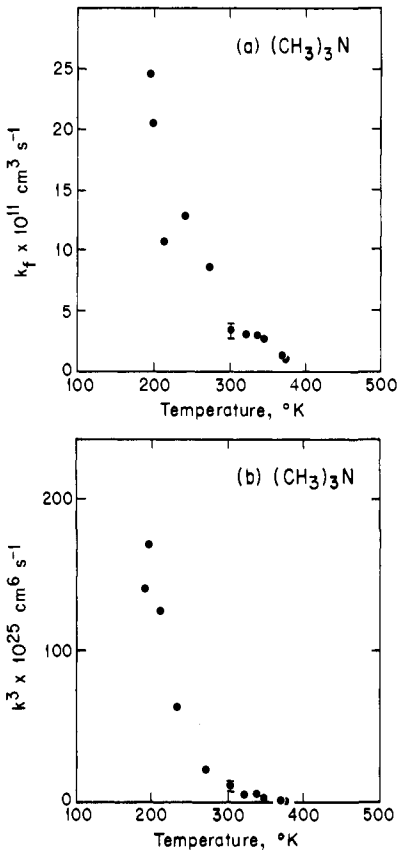

Figure 8. $(CH_3)_3N$: (a, top) plot of k_f vs. T; (b, bottom) plot of k_3 vs. T.

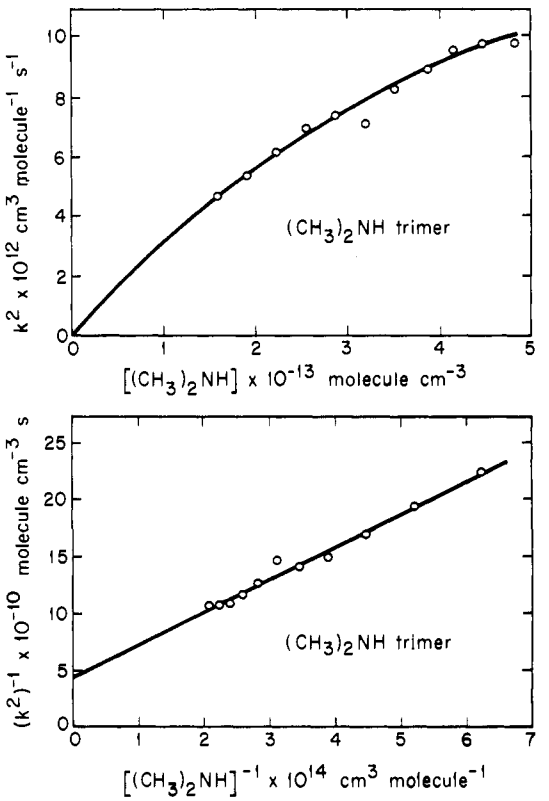

Figure 9. (a, top) Plot of the apparent second-order rate constant, k_2, vs. $[(CH_3)_2NH]$ for the formation of the trimer ion $[(CH_3)_2NH]_3H^+$ from the dimer ion $[(CH_3)_2NH]_2H^+$; $T = 302$ K. (b, bottom) Plot of $1/k_2$ vs. $[(CH_3)_2NH]^{-1}$ of the data in (a). The values of k_f and k_3 determined from the intercept and slope of this line produce the solid curve in (a) when substituted in eq 4.

lived" variety could undergo competition between collisional stabilization and fragmentation. There is ample evidence for "direct" ion–molecule reactions that proceed without the formation of a collision complex that lasts as long as the period of molecular rotation.[22] Much of the data is for small systems, but at energies above a few electron volts even large systems sometimes prefer a direct mechanism.[23]

One interpretation of the data for k_f in Table II is as follows. The reaction coordinate for formation of the complex is most probably the A_2H^+ asymmetric stretch depicted in I since the reaction complexes, in their most stable configurations, are certainly the proton bound dimers II. If the assymetric stretch depicted in I is the reaction coordinate for formation of the

$$\underset{\text{I}}{R_3N\text{-----}\ H^+\text{—}NR_3} \qquad \underset{\text{II}}{R_3N\text{—}H^+\text{—}NR_3}$$

complex, then all of the collision energy is initially in the exact vibrational mode necessary for fragmentation of the dimer. If the collision complex is to last more than one vibrational period, then the energy must be dispersed from the reaction coordinate to the (other) normal modes of the complex during the characteristic time of the collision (i.e., the "collision duration"). If the rate of energy dispersal in the complex is fast relative to the "collisional duration", then "long-lived" complexes should be formed on every collision and show a statistical lifetime characteristic of their internal energy distribution. If the rate of intramolecular energy transfer is slow relative to the collision duration, then a "long-lived" complex will be formed only occasionally.

The above qualitative argument is summarized in

$$k_f = k_{ADO}\left(\frac{k_{ET}}{k_{ET} + \tau_c^{-1}}\right) \tag{9}$$

where k_{ET} is the intramolecular energy transfer rate constant, τ_c is the "collision duration", and k_{ADO} is the overall collision rate constant (assumed calculable from ADO theory[16]). One analytic form of k_{ET} is written as[24]

$$k_{ET} \simeq \frac{2\pi}{\hbar}\sum_j |\langle\psi_{AS}|A_j|\psi_j\rangle|^2\rho_j \tag{10}$$

where ψ_{AS} is the wave function for the asymmetric stretch in the dimer excited by the collision, ψ_j is the wave function of a normal mode j other than the asymmetric stretch, ρ_j is the density of states associated with normal mode j at the energy of the collision, and A_j is the anharmonic coupling operator coupling the reaction coordinate (i.e., the asymmetric stretch) to the normal mode j. It is not possible to quantitatively evaluate this expression for the systems of interest. Qualitatively, however, it is well known that the matrix elements depend very strongly on whether or not a resonance exists between ψ_{AS} and ψ_j. Also, the direct dependence of k_{ET} on ρ_j is apparent.

The value of k_f, predicted by this model, will depend on the relative values of k_{ET} and τ_c^{-1}. Clearly k_{ET} will increase as the colliding species become more complex. Both the number of normal modes and the density of states of these modes at the energy of the collision increase as the molecule becomes larger. Rabinovitch and coworkers have experimental evidence that k_{ET} is of the order of $1\text{–}5 \times 10^{12}$ s^{-1} for some molecules containing small rings.[25] In other cases, the experimental evidence suggests that k_{ET} is somewhat larger.[1-3,25] These authors[25] suggest that the value for k_{ET} will depend on the mode of activation of the active molecule and the relationship of the activation step to other normal modes of the molecule, in particular the mode responsible for fragmentation.

The "collision duration" for ammonium ions colliding with amine neutrals can be estimated using a classical model. The relative velocity between the ion and the polarizable polar molecule can be calculated from the classical potential and is

given by[16]

$$v_r^2 = \frac{\alpha q^2}{\mu r^4} + \frac{2q\mu_D}{\mu r^2}\cos\theta \qquad (11)$$

where α and μ_D are the polarizability and dipole moment of the neutral molecule, q the charge of the ion, μ the reduced mass of the collision pair, and θ the angle between the dipole moment of the neutral molecule and the line of centers of the collision. In the dynamics of the collision, θ varies as the neutral molecule rotates in the potential field of the ion. For the simple treatment given here, a value of $\cos\theta$ will be used as calculated by ADO theory.[16]

In addition to the value of v_r calculated from eq 11, the ion and neutral have a thermal distribution of velocities. For this approximate treatment the average value, $v_0 = (8kT/\pi\mu)^{1/2}$, will be used. The final relative velocity according to this model is then

$$v = (v_0^2 + v_r^2)^{1/2} \qquad (12)$$

It should be noted that $v_r \gg v_0$ for the range of r considered here. The calculations were done by calculating v for a set of ion–neutral separations, r_i, with a step size of 1 Å. This value of v_i was taken to represent the average velocity in the range $r_i \pm 0.5$ Å. A "collision duration", τ_{ci}, was then calculated from the reciprocal of this velocity. The total "collision duration" was taken to be the sum of these incremental τ_{ci}'s. The separation, r_c, at which the collision begins was assumed to be the critical separation necessary for a capture collision to occur. This value of r_c can be readily estimated from ADO theory.[16] The resulting values of the collision duration are $\tau_c(NH_3) \simeq 4.9 \times 10^{-13}$ s and $\tau_c(CH_3NH_2) = 8.2 \times 10^{-13}$ s. It was assumed, from symmetry, that the collision diameter is $2r_c$. This model ignores the fact that both the ion and neutral have physical size; rather it assumes they pass through each other. Further, it ignores the "chemical" potential function that comes into play at short range. Both of these effects will tend to shorten the collision duration, the first by shortening the actual distance traveled by the pair during the "capture" portion of the collision and the second by increasing the relative velocity at short range. In any case, the values of τ_c calculated by this model are close to the right magnitude.

The values of τ_c calculated using the classical model are small, possibly much smaller than the competitive values of k_{ET}^{-1}. The chemical activation studies of Rabinovitch and coworkers[1-3,25] have always been on "deep welled" systems, with resulting internal energies on the order of 100–150 kcal/mol in the active molecule. Such large excitation energies lead to very, very large values for the densities of states associated with the various normal modes of the system. Hence, it is not surprising that large values of k_{ET} are observed in these studies, even in apparently unfavorable circumstances.[25] In the systems dealt with in this paper, the well depth is only 20–25 kcal/mol[26] and the corresponding densities of states are very much smaller than those of the systems described by Rabinovitch.

A further point bears mentioning. Sloane and Hase[27] have recently published a paper in which they calculated product distributions of the fragmentation of activated ClC≡CH molecules using a classical trajectory method. Their results suggested that the product distribution is strongly dependent on the initial mode of excitation in the active molecule. For example, when the initial mode of excitation was the C–H stretch, fragmentation leading to ClC≡C· + H· was the dominant reaction channel 10^{-12} s after excitation. Statistical calculations suggest this channel should have no intensity at any time owing to its very unfavorable energetics. The point of importance is that, in the studies reported here, all of the initial excitation in the $(A_2H^+)^*$ dimers is in the reaction coordinate for fragmentation of the complex. The combination of small well depth and the initial mode of excitation in the reaction coordinate thus makes these systems ideal candidates for possible nonstatistical behavior.

The calculations on τ_c suggest the collision time is only a relatively slowly varying function of mass and molecular complexity. Hence, the dramatic changes in k_f observed in going from the NH_3 system to CH_3NH_2 must be due primarily to changes in k_{ET}. This is not a surprising conclusion because $(CH_3NH_2)_2H^+$ has substantially more normal modes than $(NH_3)_2H^+$ and many of the modes are substantially lower in frequency.

An effect that is not explicitly included in the dynamical model is steric hindrance. As the groups surrounding nitrogen get bulkier, it becomes less easy to form the N–H$^+$–N bond. Such an effect is apparent in the data of Table II. For example, $k_f[(CH_3)_3N] < k_f((CH_3)_2NH)$, a result that does not agree with the trend that larger molecules exhibit larger values of k_f. Also it is worth noting that $k_f(CH_3CH_2NH_2) > k_f((CH_3)_2NH)$ and $k_f(CH_3CH_2CH_2NH_2) \gg k_f((CH_3)_3N)$. Apparently there is a specific steric effect arising from substitution on nitrogen that inhibits dimer formation. Numerous other examples of this effect are evident in Table II.

A second, and related effect, is that of molecular size itself, whether substitution is on nitrogen or on the alkyl group. As the molecule gets larger it becomes geometrically less likely that the proton on the ammonium ion will come in intimate contact with the nitrogen lone pair of the neutral amine during the collision. If the charge-dipolar and chemical forces attempting this alignment are not successful then a "long-lived" complex will not occur. It is the interplay of all of these factors that, in the dynamical model interpretation, limits the probability of successful capture to 10–20% under the most favorable circumstances.

The dependence of k_f on temperature is interesting. As displayed in Figures 6a, 7a, and 8a, k_f dramatically increases as temperature decreases. The experimental scatter is least in the $(CH_3)_2NH$ and $(CH_3)_3N$ systems. Interestingly, these systems display similar dependences of k_f on temperature. This result suggests a surprising balance between the different factors governing the magnitude of k_f as discussed in the previous paragraphs. At lowest temperatures (~200 K), $k_f/k_{ADO} = 0.15 \pm 0.05$, while, at highest temperatures (~400 K), $k_f/k_{ADO} \simeq 0.01$. The change, if any, in k_f with T for NH_3 could not be reliably studied owing to signal-to-noise problems. However, the few data that we do have (Table I) suggest that k_f may not depend strongly on T for this system. The data for CH_3NH_2 are given in Figure 6a and show considerable scatter. However, there is no doubt that k_f increases as T decreases in this system.

2. The Statistical Model. An alternative description to the association reactions reported here is based on statistical theory. One such treatment has recently been reported by Olmstead et al.,[10] who modeled the amine dimerizations by using a form of RRKM theory. The transition state chosen by these authors was assumed to be located at the ion–neutral separation corresponding to the height of the centrifugal barrier. The transition-state frequencies were essentially those of the isolated ammonium ion and amine with the exception that three free rotations were assumed between the two moieties. The frequencies of the dimer were chosen as those of the free amine with the modes associated with the nitrogen–proton bonds determined by forcing the entropy of the dimerization reaction (as calculated from statistical thermodynamics) equal to the experimental number. The rate constant for formation of the complex, k_f, was assumed to be given by ADO theory as was the stabilization rate constant k_s. Olmstead et al.[10] then calculate k_2 as a function of pressure and k_b as a function of temperature. These authors compare their calculated results with data recently reported by Meot-

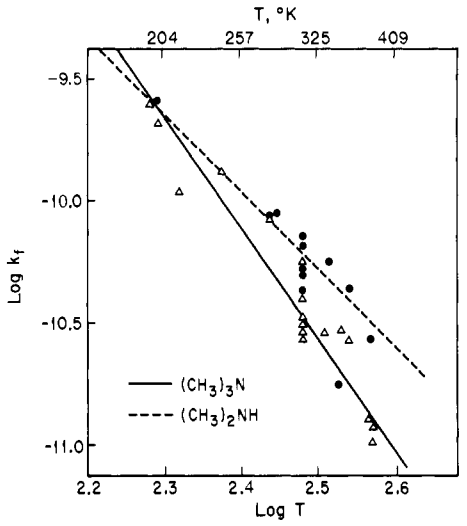

Figure 10. Plot of log k_f vs. log T; A = $(CH_3)_2NH$ (●) and A = $(CH_3)_3N$ (△).

Ner and Field[9] on the association reactions of the ammonium ions NH_4^+, $CH_3NH_3^+$, and $(CH_3)_2NH_2^+$ with their parent amines. The agreement between experiment and theory is quite good, usually within a factor of 2–3.

The data of Meot-Ner and Field[9] were taken at ~1 Torr, a pressure three orders of magnitude greater than that of the ICR experiments reported here. If the data given in this paper are extrapolated to pressures of 1 Torr, they predict that the association reactions should be pure second order in that pressure regime with values of k_2 in the 10^{-11}-cm^3/s range. Meot-Ner and Field observe that k_2 increases with pressure and the absolute magnitude of k_2 is in the 10^{-10}-cm^3/s range.

The RRKM approach suggests the high pressure data[9] and the low pressure data reported here can be reconciled because k_b, the unimolecular rate constant for fragmentation of the excited dimer, is pressure dependent. The pressure dependence of k_b arises from the pressure dependence of the energy distribution function of the fragmenting molecules: the lowest energy molecules are longest lived and are stabilized at lowest pressures while the more energetic molecules are shorter lived and are stabilized only at high pressure.

It is not possible using the theoretical results published by Olmstead et al.[10] to see if the model that they use quantitatively fits the data published here. However, they do publish a plot of k_2 vs. pressure and it is apparent from that plot that the RRKM theory will at least qualitatively fit the magnitude of the room temperature ICR data. The RRKM theory cannot reproduce the linearity of the $1/k_2$ vs. $(A)^{-1}$ plots, because of the pressure dependence of k_b, but in the pressure regime of the ICR data this dependence is expected to be slight.

The RRKM theory approach cannot explain the temperature dependence of k_f. According to this theory, as applied by Olmstead et al.,[10] k_f should always equal the collision rate constant, a term that varies only slowly with temperature.[28] The experimentally observed temperature dependence of k_f depends on the assumption that the $1/k_2$ vs. $(A)^{-1}$ plots can be extrapolated to $(A) \rightarrow \infty$. Hence, the RRKM approach argues that this extrapolation is not valid and the apparent variation of k_f with T does not have physical meaning.

Plots of log k_f vs. log T are given in Figure 10 for the $(CH_3)_2NH$ and $(CH_3)_3N$ systems. The plots are nearly linear with slopes of −3 and −5 for $(CH_3)_2NH$ and $(CH_3)_3N$, respectively. The data are collected in Table IV. The above discussion makes it clear that no certain mechanistic information can be obtained from this plot. Solomon, Meot-Ner, and Field[29] have used a form of transition-state theory to interpret data such as these, where large negative temperature coefficients are obtained. However, application of such an interpretation[29] to the association reactions considered here requires a tight transition state capable of quenching the methyl torsions of the amines. Such a transition state is unlikely in these reactions and hence the model of Solomon et al.[29] most likely can not be applied to these systems.

Table IV. Temperature Dependence of Rate Constants Written in the Form $k = CT^n$

Reaction	n
$CH_3NH_3^+ + CH_3NH_2 \xrightarrow{k_f} [(CH_3NH_2)H^+]^*$	-2 ± 2
$(CH_3)_2NH_2^+ + (CH_3)_2NH \xrightarrow{k_f} [((CH_3)_2NH)_2H^+]^*$	-3 ± 1
$(CH_3)_3NH^+ + (CH_3)_3N \xrightarrow{k_f} [((CH_3)_3N)_2H^+]^*$	-5 ± 1
$CH_3NH_3^+ + 2CH_3NH_2 \xrightarrow{k_3} (CH_3NH_2)_2H^+ + CH_3NH_2$	-4 ± 2
$(CH_3)_2NH_2^+ + 2(CH_3)_2NH \xrightarrow{k_3} [(CH_3)_2NH]_2H^+ + (CH_3)_2NH$	-5 ± 1
$(CH_3)_3NH^+ + 2(CH_3)_3N \xrightarrow{k_3} [(CH_3)_3N]_2H^+ + (CH_3)_3N$	-7 ± 1

3. Other Considerations: k_3 and k_b. The values of k_3 obtained from slopes of $1/k_2$ vs. $(A)^{-1}$ plots are tabulated in Table II and are consistent with intuitive notions for third-order rate constants. There is a steady increase in k_3 as the molecules increase in size within a particular series. The presence of steric hindrance due to substitution on nitrogen is apparent: $k_3(Me_2NH)/k_3(EtNH_2) \simeq 0.6$ and $k_3(Me_3N)/k_3(n\text{-}PrNH_2) \simeq 0.2$. These data have less scatter in them and are less prone to error than those for k_f, because they are determined by the slope of the $1/k_2$ vs. $1/(A)$ plot rather than by the intercept, which must be extrapolated.

The temperature dependence of k_3 is given in Figures 6b, 7b, and 8b for CH_3NH_2, $(CH_3)_2NH$, and $(CH_3)_3N$, respectively. This temperature dependence is very striking; for example, k_3 decreases by about a factor of 10^2 as T increases from 200 to 400 K for $(CH_3)_3N$. The plot of log k_3 vs. log T is approximately linear for this system, although there does appear to be a slight convex curvature to them analogous to the k_f data of Figure 10. From the slopes a temperature dependence of T^{-7} is determined. From our perusal of the few data that have been reported, this is the largest negative temperature exponent reported so far.[30] The data are summarized in Table IV.

There are two possible ways to obtain values for k_b, the unimolecular rate constant for fragmentation of the excited dimer. The first assumes k_f can be measured from the intercept of $1/k_2$ vs. $(A)^{-1}$ plots and the second assumes $k_f = k_{ADO}$. Both ways assume the validity of the relationship $k_b = k_f k_s/k_3$ and assume that k_s can be calculated from collision theory. A summary of these data for NH_3 and the methylamines is given in Table V. Also included are phase space theory predictions.[31] Because of the ambiguities associated with these data a detailed interpretation is not appropriate; the reaction mechanism must be determined first.

4. Comparison with Other Data. The kinetics for the dimerization reactions in NH_3, CH_3NH_2, and $(CH_3)_2NH$ have been reported by Meot-Ner and Field[9] using the technique of high pressure mass spectrometry. The results which they obtained suggest that the energy-transfer mechanism used here is appropriate, but their rate constants are in substantial quantitative disagreement with the data presented here. The values of k_2 obtained by them are generally in the range 1–10 $\times 10^{-10}$ cm^3 s^{-1}, values which are at least an order of magni-

Table V. Temperature Dependence of the Unimolecular Rate Constant, k_b, in Units of Reciprocal Seconds

	NH_3				CH_3NH_2			
T, K	Theory[a]	$k_{ADO}k_s/k_3$[b]	k_fk_s/k_3[c]	MF[d]	Theory[a]	$k_{ADO}k_s/k_3$[b]	k_fk_s/k_3[c]	MF[d]
195	2.6×10^8				0.36×10^7			
210	3.2×10^8	1.2×10^8	0.8×10^5		0.47×10^7	0.5×10^7	0.8×10^5	
278	7.3×10^8	4.4×10^8	6.0×10^5		1.3×10^7	1.1×10^7	1.6×10^5	
302	9.4×10^8	6.3×10^8	5.0×10^5		1.8×10^7	1.0×10^7	1.7×10^5	
345	14.1×10^8			2.2×10^9	3.2×10^7	2.1×10^7	1.8×10^5	1.2×10^8
370	17.5×10^8				4.4×10^7	3.3×10^7	4.2×10^5	
	$(CH_3)_2NH$				$(CH_3)_3N$			
T, K	Theory[a]	$k_{ADO}k_s/k_3$[b]	k_fk_s/k_3[c]	MF[d]	Theory[a]	$k_{ADO}k_s/k_3$[b]	k_fk_s/k_3[c]	MF[d]
195	0.21×10^6	0.2×10^6	3.2×10^4		0.05×10^6	0.09×10^6	1.4×10^4	
210	0.30×10^6				0.08×10^6	0.10×10^6	1.0×10^4	
278	1.3×10^6	0.9×10^6	6.0×10^4		0.56×10^6	0.75×10^6	4.5×10^4	
302	2.1×10^6	1.8×10^6	6.6×10^4		1.1×10^6	1.1×10^6	3.0×10^4	
345	4.8×10^6	3.9×10^6	12×10^4	6×10^7	3.5×10^6	4.5×10^6	9.5×10^4	
370	7.7×10^6	7.0×10^6	13×10^4		6.7×10^6	5.9×10^6	6.4×10^4	

[a] Phase space theory result.[31] [b] Calculated from experimental values of k_3 assuming both k_f and k_s can be calculated from ADO theory.[16] [c] Calculated from experimental values of k_3 assuming k_f is obtained by extrapolation of $1/k_2$ vs. $(A)^{-1}$ plots and k_s calculated from ADO theory.[16] [d] Data of Meot-Ner and Field.[9] At pressures and temperatures corresponding to MF's experiments the phase space theory[31] predicts $k_{ADO}k_s/k_3 = 2.0 \times 10^9$ (NH_3), 1.2×10^8 (CN_3NH_2) and 5.2×10^7 ($(CH_3)_2NH$) in excellent agreement with their numbers given in the table.

tude larger than those extrapolated from this work. They assumed k_f to be equal to the collision limit value calculated from ADO theory. By assuming that $k_s = k_{ADO}$, as is done here, they calculated values of k_b from eq 4 for a given experimental value of k_2 and (A). The values of k_b obtained by them using this technique are listed in Table V for $T = 350$ K.

There is no obvious explanation of the origins of the discrepancies between the data of Meot-Ner and Field and those reported in this paper. However, the differences in the experimental techniques used in the two laboratories may be the source of the differences. In the studies reported here, pure amines were utilized. In the work of Meot-Ner and Field,[9] however, the amines were very minor impurities (0.1 to 1%) in a chemically ionizing medium. For NH_3 the reagent gas was CH_4 (reactant ions CH_5^+ and $C_2H_5^+$) and for CH_3NH_2 and $(CH_3)_2NH$ the reagent gas was *i*-C_4H_{10} (reactant ion $C_4H_9^+$). In such mixtures, chemistry in addition to the simple protonated amine dimerization process occurs. Bennett and Field,[32] for example, have studied the ion chemistry of NH_3/CH_4 mixtures and shown the existence of the $NH_4CH_4^+$ dimer and the subsequent rapid reaction of this dimer with NH_3 to form $(NH_3)_2H^+$. Similar kinds of chemistry are also possible in the methylamine reaction mixtures. These unwanted side reactions could conceivably dominate the chemistry of the amine/reagent gas mixtures and obscure the amine dimerization kinetics of interest. Recent studies from the laboratory of Meot-Ner and Field[33] suggest this is not the case, however, and the explanation for the discrepancies between their data and the data of this paper probably lies elsewhere.

A second experimental circumstance that could effect either the data of Meot-Ner and Field or the data presented here is the problem of the approach to equilibrium. The reaction scheme for the pure amine systems is given in

$$\begin{array}{ccc} AH^+ + A & \underset{k_a}{\overset{k_f}{\rightleftharpoons}} & (A_2H^+)^* \\ \uparrow k_b & & \downarrow k_d(A) \\ (A_2H^+)^* & \underset{k_s'(A)}{\overset{k_c(A)}{\rightleftharpoons}} & A_2H^+ \end{array} \qquad (13)$$

The differential equations for this system have been solved exactly. In the limit that $k_b \simeq k_d$ and $k_s \simeq k_s'$ one obtains at equilibrium

$$k_c = k_3/K_{eq} \qquad (14)$$

The equilibrium constants, K_{eq}, have been measured by Yamdagni and Kebarle[26] for the amines of interest. Hence, from the values of k_3 reported here, values of k_c can be obtained as a function of temperature. Using these values of k_c, plots of k_2 vs. (A) can be constructed for any system approaching equilibrium. Such a plot was made for the $(CH_3)_3N$ system at 372 K. This plot bore little resemblence to the experimental plot, exhibiting much less curvature than was observed experimentally.

The effect of nonzero values of k_c on the magnitudes of k_3 and k_f was also explored. In the limit $k_d \gg k_s'(A)$ (a reasonable limit for all of the data presented here) the exact kinetic solution to scheme 13 reduces to

$$\frac{(A_2H^+)}{(AH^+)} = \frac{1 - e^{-(k_2+k_c)(A)t}}{k_c/k_2 + e^{-(k_2+k_c)(A)t}}. \qquad (15)$$

Using experimental values of (A_2H^+), (AH^+), (A), and t and values of k_c from eq 14, k_2 could be determined using iterative methods. Plots of these collisionally corrected values of k_2 vs. (A) yielded values of k_3 and k_f somewhat different from those obtained from the raw data without collisional correction. However, the maximum variation in k_3 was 9% while variations in k_f were 20–30% depending on the system. Deviations of this magnitude in k_3 and k_f do not affect the interpretation of the data discussed in previous sections of this paper.

This analysis has not been applied to the data of Meot-Ner and Field. Their experiments were performed at pressures three orders of magnitude higher than those reported here and it is possible approach to equilibrium could be occurring under those conditions.

Finally, the discrepancies between the data of Meot-Ner and Field and those presented here might be explained by an RRKM analysis such as that recently published by Olmstead et al.,[10] as previously discussed. Such an explanation is appealing because it bridges the gap between the data of Meot-Ner and Field and those presented here and it cannot be ruled out. However, it does not fit all of the details of the experimental data well and thus it cannot be unequivocally invoked as correct. More experimental data will be needed to determine the mechanism of these interesting and important reactions.

Note Added in Proof. The theoretical results reported in Table V were obtained after this paper had been submitted and reviewed. They correspond to the value of k_b calculated in the zero pressure limit. The agreement with the ICR results obtained by calculating k_b from k_sk_{ADO}/k_3 is striking. A thorough comparison of the theoretical and experimental results

is in preparation,[31] including theoretical plots of k_2 vs. A. These preliminary results suggest the statistical theory approach may well be appropriate for these systems, but the more complete analysis, in progress, is necessary to confirm this suggestion.

Acknowledgment. The support of the National Science Foundation under Grants CHE74-18397 and CHE77-15449 is gratefully acknowledged. We also gratefully acknowledge the receipt of manuscripts before publication from M. Meot-Ner and F. H. Field, and from W. N. Olmstead and J. I. Brauman. A number of extensive discussions with these authors is also gratefully acknowledged. Extensive discussions with H. Metiu and R. N. Rosenfeld are also acknowledged.

References and Notes

(1) Rabinovitch and co-workers have been primarily responsible for the development of this area. See, for example, L. D. Spicer and B. S. Rabinovitch, *Annu. Rev. Phys. Chem.*, **21**, 349 (1970), and references therein; J. H. Current, B. S. Rabinovitch, C. A. Heller, and A. S. Gordon, *J. Chem. Phys.*, **39**, 3535 (1963); J. H. Current and B. S. Rabinovitch, *ibid.*, **40**, 274 (1964); Y. N. Lin and B. S. Rabinovitch, *J. Phys. Chem.*, **74**, 3151 (1970).
(2) W. A. Forst, "Theory of Unimolecular Reactions", Academic Press, New York, N.Y., 1973.
(3) P. J. Robinson and K. A. Holbrook, "Unimolecular Reactions", Wiley-Interscience, London, 1972.
(4) R. A. Marcus and O. K. Rice, *J. Phys. Colloid. Chem.*, **55**, 894 (1951); R. A. Marcus, *J. Chem. Phys.*, **20**, 359 (1952). See also ref 2 and 3.
(5) See, for example, J. M. Parsons, K. Shobotake, Y. T. Lee, and S. A. Rice, *Faraday Discuss. Chem. Soc.*, **55**, 344 (1973), and references therein.
(6) P. S. Gill, Y. Inel, and G. G. Meisels, *J. Chem. Phys.*, **54**, 2811 (1971).
(7) D. K. Bohme, D. B. Dunkin, F. C. Fehsenfeld, and E. E. Ferguson, *J. Chem. Phys.*, **49**, 5201 (1968); **51**, 863 (1969).
(8) V. G. Anicich and M. T. Bowers, *J. Am. Chem. Soc.*, **96**, 1279 (1974).
(9) M. Meot-Ner and F. H. Field, *J. Am. Chem. Soc.*, **97**, 5339 (1975).
(10) W. N. Olmstead, M. Lev-On, D. M. Golden, and J. L. Brauman, *J. Am. Chem. Soc.*, **99**, 992 (1977).
(11) (a) V. G. Anicich and M. T. Bowers, *Int. J. Mass Spectrom. Ion Phys.*, **11**, 329 (1973); V. G. Anicich, Ph.D. Thesis, University of California, Santa Barbara, Calif., 1973. (b) M. T. Bowers, P. V. Neilson, P. R. Kemper, and A. G. Wren, *Int. J. Mass Spectrom. Ion Phys.*, **25**, 103 (1977).
(12) T. B. McMahon and J. L. Beauchamp, *Rev. Sci. Instru.*, **42**, 1632 (1971).
(13) A. G. Wren, P. G. Gilbert, and M. T. Bowers, *Rev. Sci. Instrum.*, **49**, 531 (1978).
(14) P. R. Kemper and M. T. Bowers, *Rev. Sci. Instrum.*, **48**, 1477 (1977).
(15) D. P. Ridge and J. L. Beauchamp, *J. Chem. Phys.*, **64**, 2735 (1976).
(16) T. Su and M. T. Bowers, *J. Chem. Phys.*, **58**, 3027 (1973); T. Su and M. T. Bowers, *Int. J. Mass Spectrom. Ion Phys.*, **12**, 347 (1973); L. Bass, T. Su, W. J. Chesnavich, and M. T. Bowers, *Chem. Phys. Lett.*, **34**, 119 (1975).
(17) See, for example, J. L. Beauchamp, *Annu. Rev. Phys. Chem.*, **22**, 527 (1971).
(18) M. B. Comisarow, *J. Chem. Phys.*, **55**, 205 (1971).
(19) P. R. Kemper, Ph.D. Thesis, University of California, Santa Barbara, Calif., 1977.
(20) J. M. Brupbacher, C. J. Eagle, and E. Tschuikow-Roux, *J. Phys. Chem.*, **79**, 671 (1975).
(21) G. Giomousis and D. P. Stevenson, *J. Chem. Phys.*, **29**, 294 (1958).
(22) See, for example, Z. Herman, J. Kerstetter, T. Rose, and R. Wolfgang, *Discuss. Faraday Soc.*, **44**, 123 (1967); W. R. Gentry, E. A. Gislason, Y. T. Lee, B. H. Mahan, and C. W. Tsao, *ibid.*, **44**, 137 (1967); W. R. Gentry, E. A. Gislason, B. H. Mahan, and C. W. Tsao, *J. Chem. Phys.*, **49**, 3058 (1968); E. A. Gislason, B. H. Mahan, C. W. Tsao, and A. S. Werner, *ibid.*, **50**, 142 (1969).
(23) Z. Herman, A. Lee, and R. Wolfgang, *J. Chem. Phys.*, **51**, 452 (1969).
(24) L. I. Schiff, "Quantum Mechanics", 2nd ed, McGraw-Hill, New York, N.Y., 1958, p 199.
(25) J. D. Rynbrandt and B. S. Rabinovitch, *J. Chem. Phys.*, **54**, 2275 (1971); A. N. Ko, B. S. Rabinovitch, and K. J. Chao, *ibid.*, **66**, 1374 (1977).
(26) R. Yamdagni and P. Kebarle, *J. Am. Chem. Soc.*, **95**, 3504 (1973).
(27) C. S. Sloane and W. L. Hase, *J. Chem. Phys.*, **66**, 1523 (1977).
(28) T. Su and M. T. Bowers, *Int. J. Mass Spectrom. Ion Phys.*, **17**, 211 (1975).
(29) J. J. Solomon, M. Meot-Ner, and F. H. Field, *J. Am. Chem. Soc.*, **96**, 3727 (1974).
(30) Many data are summarized by R. F. Porter, "Interactions Between Ions and Molecules", P. Ausloos, Ed., Plenum Press, New York, N.Y., 1975. Meot-Ner and Field[9] have also reported a temperature dependence of about T^{-7} for amine dimerization reactions.
(31) L. Bass, W. J. Chesnavich, and M. T. Bowers, unpublished work.
(32) S. L. Bennett and F. H. Field, *J. Am. Chem. Soc.*, **94**, 6305 (1972).
(33) M. Meot-Ner, private communication.

Generalized Selection Rules: Symmetry Rules for Molecules or Chromophores in Perturbing Fields

Pieter E. Schipper

Contribution from the Department of Theoretical Chemistry, The University of Sydney N. S. W. 2006, Australia. *Received November 2, 1977*

Abstract: Generalized selection rules are developed for any interaction process involving a species of given symmetry in the presence of perturbing fields (such as static electric and magnetic or radiation fields, or that due to the presence of another species). It is suggested that the selection rules be defined in two stages: those giving the combinations of operators allowed under the symmetry of the species (operator selection rules) and those giving the allowed intermediate states (state selection rules). The former are shown to reduce to the symmetry rules of the classical tensor describing the molecular response, and lead to the concept of an invariant operator characteristic of the point group of the molecule corresponding to the classical tensorial observable. The method is illustrated by application to some simple interaction processes.

Introduction

Selection rules are of such fundamental importance and widespread use in chemistry that it is easy to overlook that they are basically of two quite distinct types: classical selection rules (which are essentially the symmetry rules describing the conditions under which the classical observable must vanish under the molecular symmetry) and quantum mechanical selection rules (which are the corresponding symmetry rules for the matrix elements in the quantum mechanical expressions describing the same process). We can illustrate this with recourse to the familiar concept of polarizability.

The interaction of a molecule A with an electrostatic field $\mathbf{E}$ leads to the following *classical* expression for the resultant induced dipole moment of A:

$$\delta\boldsymbol{\mu} = \hat{\alpha}^{c}\mathbf{E} \tag{1}$$

$\hat{\alpha}^{c}$ is the classical polarizability tensor with elements α^{c}_{ij}, where i,j are Cartesian indexes. If the molecule has a symmetry higher than C_1 (containing only the identity), certain elements of the polarizability tensor will be related by symmetry, or vanish. Definition of these conditions lead to the classical tensor selection rules, which have been discussed in some detail by Birss[1] in a monograph directed at solid state problems. The *quantum* equivalent of the above expression has the form

0002-7863/78/1500-3658$01.00/0